R-18

THE ABSOLUTE PHOTOMETRY OF THE ZODIACAL LIGHT

L. L. Smith, F. E. Roach[*] and R. W. Owen

Central Radio Propagation Laboratory
National Bureau of Standards, Boulder, Colorado

and

Hawaii Institute of Geophysics
University of Hawaii, Honolulu, Hawaii

29493

Abstract—Interpretation is made of photometric records
obtained at the Haleakala Observatory during six nights
between August 1961 and June 1962. An interference
filter centered on wavelength 5300 A was used. After
allowance for the airglow continuum and the integrated
starlight, the residual is interpreted as due to
zodiacal light. The brightness of the zodiacal light
is tabulated for that part observable in the night
sky. Graphical representations illustrate the dis-
tribution of brightness in ecliptic coordinates.

I. INTRODUCTION

As a part of the airglow-zodiacal light program of the Haleakala

Observatory of the Hawaii Institute of Geophysics (latitude N 20°.7,

longitude W 156°.16), a photometer having an interference filter

centered on wavelength 5300 A was used in systematic observations of

the night sky during the period from May 1961 to September 1962.

---

[*]The paper was prepared while FER was the recipient of a

Senior Research Scholarship at the East-West Center of the University

of Hawaii.

The observing program involved scanning the sky in a series of
almucantars at zenith distances 80°, 75°, 70°, 60°, 40° plus the
zenith. In addition to the photometer (designated by us as RP),
the alt-azimuth mount carried (a) a birefringent filter photometer
for the study of the night airglow [1] and (b) a polarimeter-photometer
used by J. L. Weinberg[2] for a detailed study of the polarization
(and photometry) of the zodiacal light. An auxiliary zenith photometer
having a built-in and absolutely calibrated standard light was oper-
ated during all the observations[3] making it possible to obtain the
calibration of the RP photometer by comparison of the simultaneous
zenith sky readings throughout a night.

II. THE OBSERVATIONAL MATERIAL

The six nights included in the study (Table 1) were distributed
throughout the year in approximately 2-month intervals. The principal
reason for such a spread was to give a complete coverage of the
astronomical sky for a photometric study of the integrated starlight
especially in the Milky Way. /the present study, we have avoided
galactic latitudes less than 30° in order to minimize uncertainties
due to corrections for integrated starlight. Subsequently, we plan
to return to the Milky Way study.

The large ensemble of data (more than one million individual readings) resulted in a library of print-outs of the absolute brightness of the night sky referred to outside the atmosphere for each degree of the sky and for the several almucantars involved in each sky survey.

The data have been examined in both systematic and specialized ways. An example of systematic use was the plotting of the 40° zenith distance readings for each half hour of sidereal time. An example of a specialized use of the data was the detailed coverage of the region near the ecliptic pole for which plots for each 5-minute survey were made over an extended period in order to delineate the details. We have been able to make corrections for errors in azimuth settings by comparison of peaks of maximum star deflections with their computed azimuths. Based on such comparisons, we believe that an individual azimuth is known to about ± 5°, not good enough for any finesse concerning the photometric axis of the zodiacal light but consistent with the 4° field of view of the photometer. Our final results based on a large quantity of data are probably good to ± 2° in the various coordinates.

We have referred the readings to outside the atmosphere by allowing for (a) the extinction of the lower atmosphere plus ozone, (b) the scattering of the lower atmosphere and (c) the increase of

the airglow component toward the horizon. Some comment is in order
on the problem of correcting for scattered light. We have used the
tables by Ashburn[4] who made numerical integrations of Rayleigh
scattering for (a) a uniform sky with all the light coming from
astronomical sources (assumed to be at an infinite distance) and
(b) an emitting layer in the upper atmosphere, uniform as seen from
the center of the earth but not uniform as seen from the earth's
surface. The problem of coping with a non-uniform sky has not been
solved (except for the special case of a single point source such as
the sun) and, therefore, the use of the Ashburn tables introduces
some errors, fortunately small, when applied to an actual sky in
which both the astronomical (zodiacal light, Milky Way) and the
airglow (dependence on azimuth) components are not uniform.

The principal difficulty in practice is that the Ashburn
constants require multiplication by an average sky brightness as
seen outside the scattering atmosphere. It is not possible to
utilize for this purpose any particular region of the sky such as
the zenith which is frequently strongly affected by the Milky Way.
We have, therefore, made an estimate of the "average" sky brightness,
J, for purposes of obtaining the scattering correction by an approxi-
mation technique. This is best shown by indicating analytically our
data processing procedure. We define the following quantities:

z = zenith distance,

A = azimuth,

m(z) = air mass from Haleakala,

τ_1 = extinction coefficient to refer a reading to outside the atmosphere,

τ_2 = extinction coefficient to refer a reading to outside the lower atmosphere but just inside the ozone layer,

τ_3 = molecular (Rayleigh) coefficient,

J = average brightness of a uniform sky corresponding to the actual non-uniform sky just inside the ozone layer,

Sc(z) = scattering factor from Ashburn's tables to be multiplied into J,

V(z) = the van Rhijn function giving the increase with zenith distance of an airglow layer as seen from the surface of the earth,

R(z,A) = the observed reading at z and A,

L(z) = the slant brightness in reading units of the sky just inside the ozone layer.

The observed brightness in reading units can be defined as

$$R(z,A) = L(z)e^{-\tau_2 m(z)} + Sc(z) \cdot J. \tag{1}$$

Assuming the upper atmosphere component of J as 25% and the infinity
component as 75%[*], then

$$L(z) = .25 \cdot V(z) \cdot J + .75 \cdot J. \tag{2}$$

Substituting L(z) from equation (2) into equation (1), we find

$$J = R(z,A)/[(.25 \cdot V(z) + .75)e^{-\tau_2 m(z)} + Sc(z)]. \tag{3}$$

J was determined for each survey by computing it for each zenith
distance and azimuth observed and taking the average of the 1800
(360 azimuth readings for each of 5 zenith distances) computations.
Finally, we arrive at an expression for the brightness in absolute
units $[S_{10}(vis)]$ outside the atmosphere by the formula

$$I(o/a) = [R(z,A) - Sc(z)J]e^{\tau_1 m(z)} \cdot Q \tag{4}$$

where Q is the calibration constant to refer our galvanometer readings
to $S_{10}(vis)$ units of brightness. For a discussion of the $S_{10}(vis)$

---

[*]The scattering correction is relatively insensitive to the
assumed percentage of infinity and atmospheric light. As we have later
determined (Table 4), it would have been better to have used a lower
percentage for the airglow component. We did not repeat the calcula-
tions to correspond to the deduced percentages of airglow (Table 4)
since the effect on the final result would have been small.

unit and of the methods we have used to evaluate Q, we refer to Roach and Smith[5]. Table 2 is a summary of the constants used in equations (3) and (4).

III. THE INTEGRATED STARLIGHT

As mentioned above, we avoided regions of the sky with galactic latitudes smaller than 30°*. In a recent study, Roach and Smith[5] concluded that the integrated starlight for high galactic latitudes deduced from the Groningen 43[6] star counts [see Roach and Megill[7]] represents the true integrated starlight when multiplied by 1.26. In the present study, we have taken 1.26 times the integrations from Groningen 43 for our estimations of the photometric effect of the integrated starlight. A point by point evaluation of the integrated starlight was made by a double interpolation between the values obtained from the tabular entries in Groningen 43.

The magnitude of the integrated starlight corrections is indicated in Table 3 in which the average values are given for selected galactic latitudes.

---

*The single exception is the ecliptic pole for which the galactic latitude is 28°.

IV.   THE AIRGLOW CONTINUUM

The filter of our photometer was chosen so as to avoid any bright airglow emissions. Nevertheless, the presence of an airglow "continuum" in our observations is indicated by the systematic increase of the measured intensities toward the horizon. Such an increase has long been associated with the presence of an airglow component in the observations (the so-called van Rhijn effect). In a later study, we propose to go into the airglow problem in detail and here record in Table 4 the absolute airglow brightness used for each of the nights in the present analysis.

The airglow continuum was as much as 24% of the total light (J), but that this percentage does change significantly from night to night is indicated by the spread in the values listed in Table 4. Changes during a night and variations of brightness with azimuth were ignored in our treatment and errors due to ignoring these changes contribute slightly to the scatter in our final results. We refer to such errors as "subtractive" since they arise from uncertainties in subtracting out the non-zodiacal light components.

V.   THE OBSERVATIONAL RESULTS

The numerical results of our study are assembled in Table 5 in the form of zodiacal light brightnesses over the observable domain

with $5°$ intervals in the parameters ecliptic latitude, β, and the differential ecliptic longitude, $\lambda - \lambda_\odot$.

In Fig. 1 the ensemble of data is plotted as isophotes in polar coordinates, β and $\lambda - \lambda_\odot$. The center of the plot is the ecliptic pole and the periphery is the ecliptic. In our analysis, we have averaged evening and morning results which correspond to the upper and lower parts of the plot which are thus mirror images of each other.

VI. DISCUSSION

The gross characteristic that stands out from an inspection of Fig. 1 is the contrast between the left and right halves of the plot. The right half represents intensities due to light originating from the dark or night side of the earth if one considers the problem in its diurnal context. It is probably preferable to consider it as a solar system problem and in this sense the right half of the plot is due to light from beyond the earth's orbit. The gegenschein shows as a small enhancement at $\lambda - \lambda_\odot = 180$. There is a steady decline in brightness toward the ecliptic pole, but the distortion of the isophotes just on the sunward side of the pole gives an illusion that the center of the photometric minimum is not centered on the pole itself. On the left side of the plot, a dramatic increase of brightness is noted. The very bright zodiacal light $[> 1000 \; S_{10}(vis)]$ is brighter than most of our present observations and is shown without structure.

We show in Fig. 2 a plot of the zodiacal light brightness as a function of the ecliptic latitude for a differential ecliptic longitude, $\lambda - \lambda_\odot$, of 90°, a value chosen since it corresponds to a constant elongation, ϵ , of 90° over the whole plot[*]. The brightness goes steadily down from 250 S_{10}(vis) at the ecliptic to 110 S_{10}(vis) at the pole.

In Fig. 3 we show the brightness of the zodiacal light as a function of ϵ for two cases: (a) in the plane of the ecliptic where $\epsilon = \lambda - \lambda_\odot$, and (b) perpendicular to the plane of the ecliptic where $\epsilon = \beta$ for $\lambda - \lambda_\odot = 0°$ up to $\beta = 90°$ and where $\epsilon = 180° - \beta$ for $\lambda - \lambda_\odot = 180°$. The two curves come together at the gegenschein ($\epsilon = 180°$) and would do so at the sun ($\epsilon = 0°$) if we were able to carry our observations to that direction in space.

An interesting empirical quantity is the ratio, P, of the brightness of the zodiacal light at a given elongation in the ecliptic to that at the same elongation in a plane perpendicular to the ecliptic. For $\epsilon = 90°$ we note that $P = \frac{250}{110} = 2.27$. We have attempted to make an <u>approximate</u> evaluation of P over the domain from the sun to the gegenschein based on a number of published sources plus the observations of this study. The last row (for $\lambda - \lambda_\odot = 0°$) in Table 5

─────────────────────

[*]The elongation, ϵ , is conveniently derived from the expression: $\cos \epsilon = \cos (\lambda - \lambda_\odot) \cos \beta$.

contains a number of entries in parentheses* which represent
graphical extrapolations down each column. These numbers are
included in Table 6 in the column headed "Brightness, $\perp$ ecliptic".
The three entries in the "in ecliptic" column for 15°, 20° and 25°
elongation are from Table III in Ingham[8] with a factor of 1.20
found empirically necessary to put his observations into our scale**.

The ratio, P, must necessarily be unity at elongations of 0°
(the sun) and 180° (the gegenschein). Any photometric concentration
toward the ecliptic requires that the ratio be greater than one at
intermediate elongations. An inspection of Fig. 4 indicates a
maximum ratio of almost 5 at an elongation of 35°. We suggest that
a refinement of Fig. 4 might be an interesting observational goal.

In the region between $\epsilon = 50°$ and 90° in the plot of Fig. 4,
a departure of P from the smooth curve (as dashed by us) is noted.

---

*The quantities within parentheses in the first two columns
also represent graphical extrapolations, but in this case, the reason
for the extrapolation was to attempt to allow for the slow time
response of our recording galvanometer.

**Example: At $\epsilon = 35°$, Ingham records a brightness of $\underline{1390}$
compared to our value of $\underline{1595}$.

When this came to our attention in the early examination of the data, we made a concentrated study of the region. Inspection of Fig. 1 demonstrates that the photometric irregularity seems to persist away from the $\lambda - \lambda_\odot = 0°$ domain as evidenced by the 200 S_{10}(vis) islands near $\beta = 55°$ and $\lambda - \lambda_\odot = 45°$ (corresponding to $\epsilon = 66°$). We cannot detect any such perturbation extending down to the ecliptic in the $\epsilon = 65°$ ($\lambda - \lambda_\odot = 65°$ also) region*. It should be remarked that the region of enhancement was included in our records over almost a 4-month period from August 14/15 to November 6/7, 1961, a period during which the position of the Milky Way in the sky permitted a definitive test.

In order to indicate the evidence for the excess which led to the S_{10}(vis) = 200 islands in Fig. 1, we show in Fig. 5 plots of the brightness versus differential elongation for a family of values of β from 25° to 80°. The region of excess is seen as a progression of maxima especially in the curves for $\beta = 45°$, 50° and 55°. In Fig. 6 we have isolated the excess in the plane perpendicular to the ecliptic based on the departure of the distorted region (Fig. 4) from the smooth curve (dashed) indicating a brightness of some 50 S_{10}(vis) units.

---

*In a detailed plot of the zodiacal light brightness in the ecliptic by Weinberg[2], there is a hint of a slight enhancement in the $\epsilon = 65°$ region.

We assume the privilege of the observer to be the first to speculate about the physical significance of his own observations and suggest that the excess may be due to a concentration of scattering material some 50° to 90° from the sun in the general region away from the ecliptic. If this be the explanation then a localized (with respect to the earth) concentration seems to us more reasonable than one extending over some 120° of ecliptic longitude over the four months that the excess was observed.

VII. CONCLUSIONS

From systematic photometric observations of the night sky at the Haleakala Observatory, we have isolated the zodiacal light component and recorded it in terms of ecliptic coordinates. We find a photometric ecliptic enhancement of 4.88 at its maximum for an elongation of 35° and of 2.27 at an elongation of 90°. We find evidence for a photometric perturbation some 70° from the sun in regions well away from the ecliptic.

VIII. ACKNOWLEDGMENTS

It is a pleasure to acknowledge the help we have received from several colleagues in the prosecution of this study. We are indebted to Mr. H. M. Mann and to Mr. H. Tanabe for obtaining the original photometric records; to Dr. Robert Sparks for assistance

REFERENCES

1. D. Barbier, F. E. Roach, and W. R. Steiger, J. Research NBS 66D, 145 (1962).

2. J. L. Weinberg, PhD. dissertation, University of Colorado (1963).

3. C. M. Purdy, L. R. Megill, and F. E. Roach, J. Research NBS 65C, 213 (1961).

4. E. V. Ashburn, J. Atmospheric Terrest. Phys. 5, 83 (1954).

5. F. E. Roach and L. L. Smith, NBS Tech. Note 214 (1964).

6. P. J. van Rhijn, Groningen Publication No. 43 (1925).

7. F. E. Roach and L. R. Megill, Astrophys. J. 133, 228 (1961).

8. M. F. Ingham, Monthly Notices Roy. Astron. Soc. 122, 157 (1961).

9. F. E. Roach and A. B. Meinel, Astrophys. J. 122, 530 (1955).

10. C. W. Allen, Astrophys. Quant. p. 116 (1955).

11. R. Michard, A. Dollfuss, J. C. Pecker, M. Laffineur, and Mme. M. d'Azambuja, Ann. d'Astrophys. 17, 4 (1954).

Table 1

The Six Nights Included in this Study

Night	Period of Observations				Number of Sky Surveys
	Beginning		End		
	H.S.T. (hrs.:mins.)	Sid Time (degrees)	H.S.T. (hrs.:mins.)	Sid Time (degrees)	
1961					
Aug. 14/15	21:00	272	04:55	31	96
Sept. 11/12	19:40	280	04:55	59	112
Nov. 6/7	22:55	23	05:30	122	79
1962					
Feb. 3/4	19:45	63	05:30	210	117
March 31/ Apr 1	19:50	120	04:10	245	99
June 27/28	20:30	217	03:20	319	82
					585 (total)

Table 2

Constants Used in the Reduction of the Data

z	m(z)	τ			$\tau_n(z)$			$e^{\tau_n(z)}$		Sc(z)	V(z) h=100km
		$\tau_1^{(1)}$	$\tau_2^{(2)}$	$\tau_3^{(3)}$	$\tau_1 m(z)$	$\tau_2 m(z)$	$\tau_3 m(z)$	for $\tau_1 m(z)$	for $\tau_2 m(z)$		
0	0.684	0.142	0.121	0.112	0.097	0.083	0.077	1.102	1.087	0.047	1.000
40	0.839	"	"	"	0.126	0.108	-	1.135	1.114	0.061	1.292
60	1.363	"	"	"	0.194	0.166	-	1.214	1.181	0.093	1.914
70	1.984	"	"	"	0.282	0.240	-	1.326	1.271	0.131	2.635
75	2.613	"	"	"	0.371	0.316	-	1.449	1.372	0.163	3.234
80	3.830	"	"	"	0.544	0.463	-	1.723	1.589	0.238	4.055

(1) From Weinberg(2).

(2) $\tau_2 = \tau_1 - .021$ (ozone absorption, Roach and Meinel(9)).

(3) From Allen(10).

TABLE 3

Mean Integrated Starlight

Galactic Latitude	Mean Integrated Starlight (from Groningen 43) in S_{10}(vis) units	Mean Integrated Starlight used (1.26 X GR 43)
80	31.1	39.2
70	32.5	41.0
60	35.5	44.7
50	41.3	52.0
40	51.5	64.9
30	68.7	86.6

Table 4
The Airglow Continuum

| Date | Airglow Continuum ($S_{10}(vis)$) | | | | | | | Mean | Percent Airglow zenith |
	z = 0	40	60	70	75	80		J	Mean J
1961									
Aug 14/15	60	75	115	160	195	255		285	21
Sep 11/12	60	75	115	160	195	260		305	20
Nov 6/7	80	100	155	215	265	355		330	24
1962									
Feb 3/4	20	25	40	55	65	85		245	8
Mar 31/Apr 1	45	60	95	130	160	210		300	17
Jun 27/28	50	65	100	140	170	225		305	16

Table 5

Brightness of the Zodiacal Light in Ecliptic Coordinates

λ-λ☉ \ β	90	85	80	75	70	65	60	55	50	45	40	35	30	25	20	15	10	5	0
180	110		115	115	115	125	125	125	125	130	125	140	150	155	165	175	135	195	205
175			115	115	115	125	125	125	125	130	125	135	150	150	160	165	175	190	195
170			115	115	115	125	125	125	120	130	125	135	145	150	155	160	170	175	185
165			115	115	115	125	125	125	120	130	125	135	145	145	150	160	165	170	175
160			115	115	115	125	125	120	125	130	125	135	145	145	145	155	150	170	175
155			115	115	115	125	125	125	125	130	125	135	145	145	150	155	160	165	170
150			110	115	115	125	125	125	125	130	125	140	145	150	150	155	160	165	170
145			110	115	115	125	125	125	130	135	125	140	145	155	155	155	165	170	175
140			115	115	115	125	125	120	130	135	130	140	145	155	155	160	165	170	175
135			115	115	115	125	125	120	135	135	135	145	145	155	160	160	170	170	175
130			115	115	115	125	125	125	135	135	135	145	150	160	160	165	170	175	175
125			115	115	115	125	125	125	135	135	135	145	150	160	165	165	175	175	180
120			115	115	120	125	125	125	135	135	135	145	150	160	165	170	180	180	185
115			115	115	120	125	125	125	135	135	135	150	155	165	170	175	180	185	190
110			115	115	115	125	125	125	135	135	140	150	155	165	170	175	185	190	200
105			120	115	115	120	125	130	135	135	145	150	160	170	175	175	190	200	210
100			120	115	120	125	125	130	135	135	145	150	165	170	175	180	195	205	220
95			125	120	120	125	125	130	135	135	150	155	185	175	180	190	205	215	235
90			125	125	120	125	125	130	135	135	150	160	205	180	185	200	215	235	250
85			130	125	125	125	125	130	140	145	155	165	205	190	195	215	235	255	265
80		110	130	130	125	125	125	130	140	150	155	170	215	200	210	230	255	275	290
75		110	130	130	130	125	135	130	150	165	160	175	225	210	225	245	285	300	320
70		115	130	130	130	125	140	140	165	195	175	185	230	225	240	265	310	335	(370)
65		115	130	135	130	125	145	145	180	200	200	205	240	240	255	285	345	370	(425)
60		115	135	135	130	135	140	160	205	195	205	205	250	255	270	305	380	425	(500)
55		120	135	135	135	140	145	170	205	190	205	205	270	285	290	330	430	505	(600)
50		120	135	135	140	145	155	190	195	190	205	205	300	315	315	370	485	610	(745)
45		120	135	135	140	150	160	205	185	190	210	215		360	345	425	555	735	(945)
40		125	135	135	140	150	170	200	180	195	215	220		410	390	505	655	870	(1185)
35		125	130	175	185	170	185	200	185	190	215	225	230	465	450	690	845	(1145)	(1595)
30		125	130	130	175	175	185	190	195		220	230		520	545	905			(2330)
25			130	125	150	175	190	190	175	200	225	245							
20		135	145	145	150	170	190	185	180	205	230								
15			150	155	155	185	185	180	180	205	235								
10			150	155	155	185	185	175	180	210									
5			150	160	155	185	185	175	175	(215)									
0		(135)	(150)	(160)	155	(185)	(185)	(175)	(180)	(215)	(250)	(330)	(525)	(995)	(1820)	(6150)			

Table 6

Brightness of the Zodiacal Light in the Plane of the
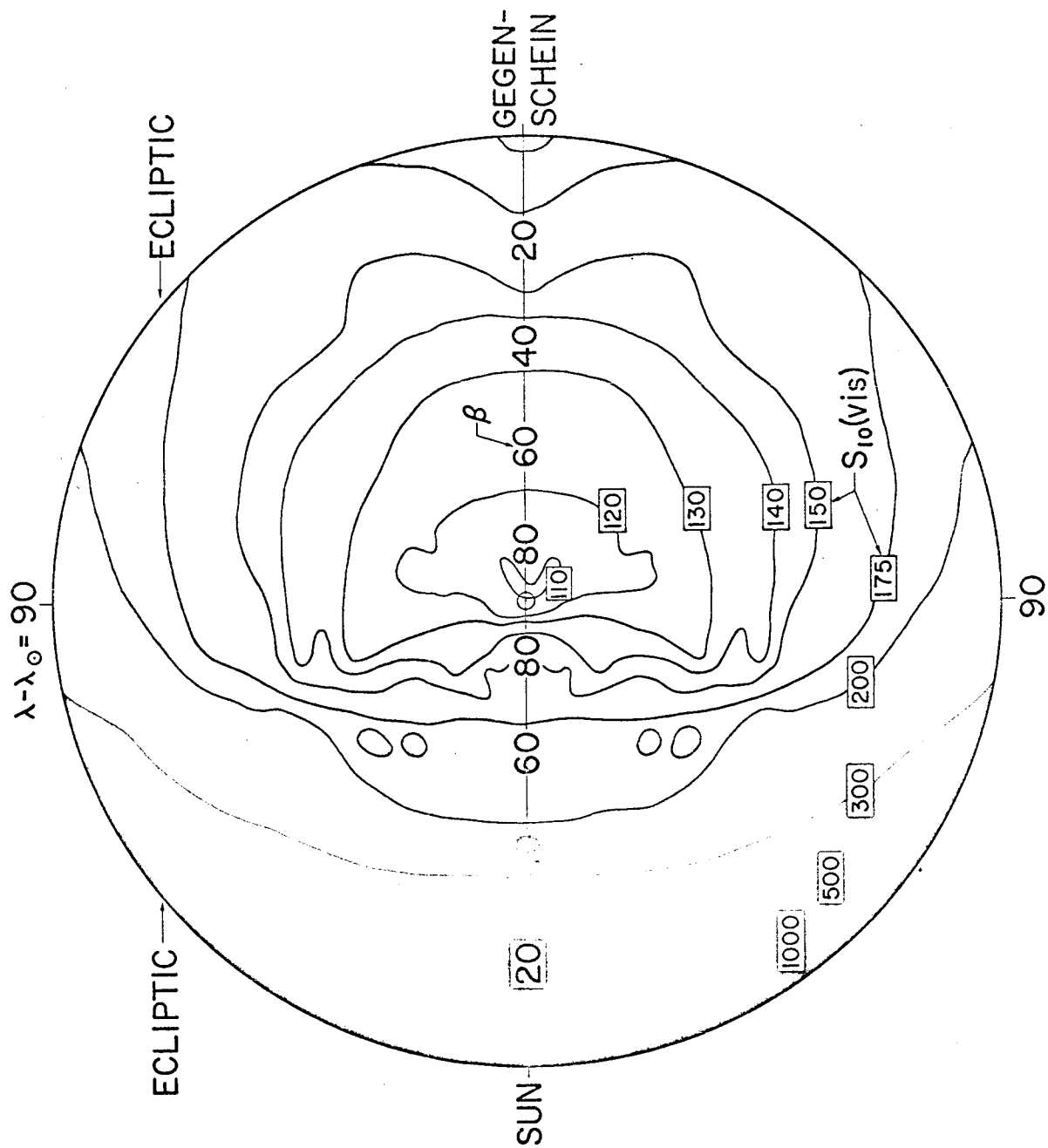Ecliptic and in a Plane Perpendicular to the Ecliptic

Elongation, ε	Brightness, S_{10}(vis)		Ratio, P.
	In ecliptic	⊥ ecliptic	
2.4°	966,400*	634,300*	1.52
5.20°	240,200*	137,600*	1.75
15	13,800**	6150	2.24
20	6200***	1820	3.41
25	3640***	995	3.66
30	2330	525	4.44
35	1595	330	4.88
40	1185	250	4.74
45	945	215	4.40
50	745	180	4.14
55	600	175	3.43
60	500	185	2.70
65	425	185	2.30
70	370	155	2.39
75	320	160	2.00
80	290	150	1.93
85	265	135	1.96
90	250	110	2.27

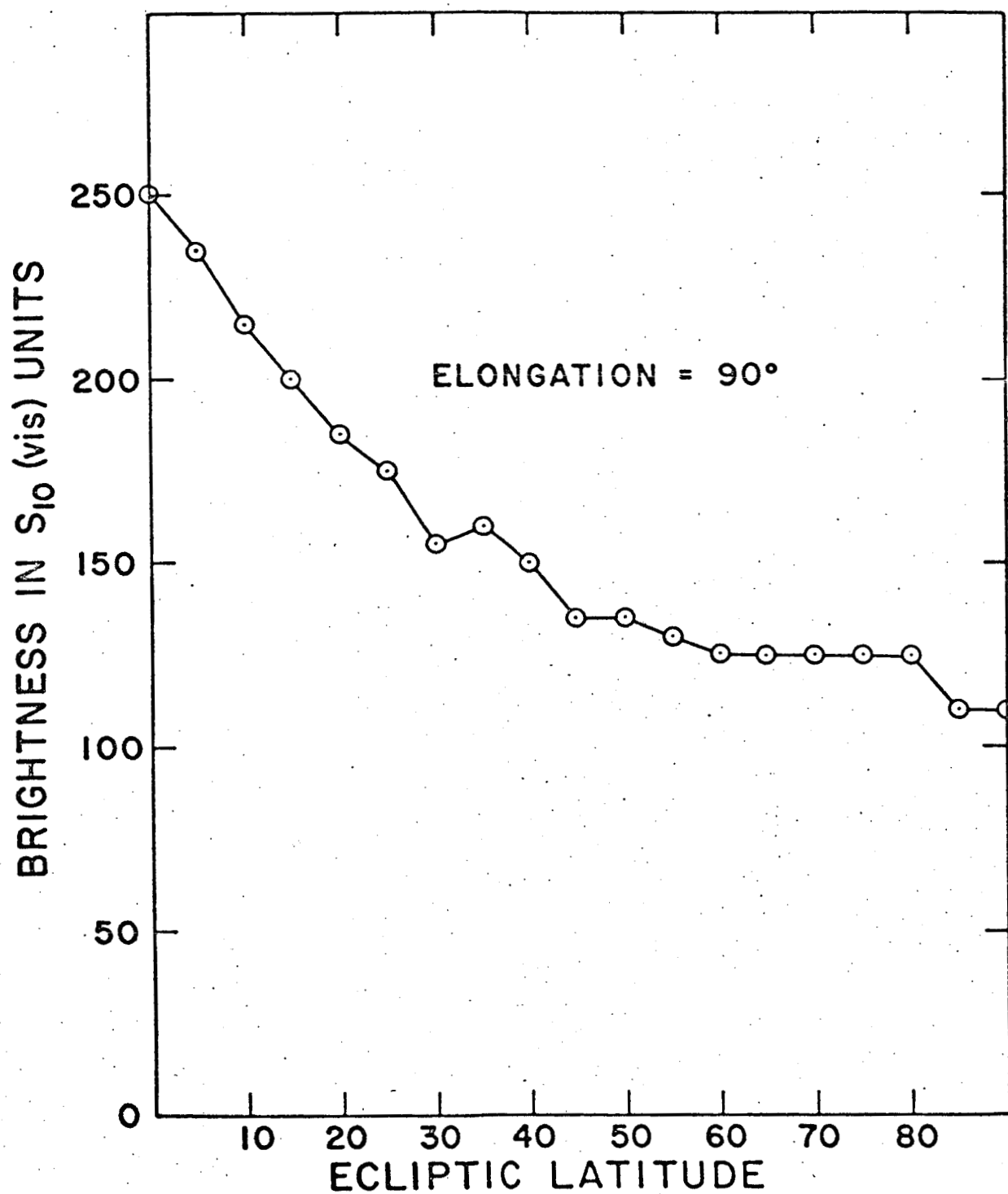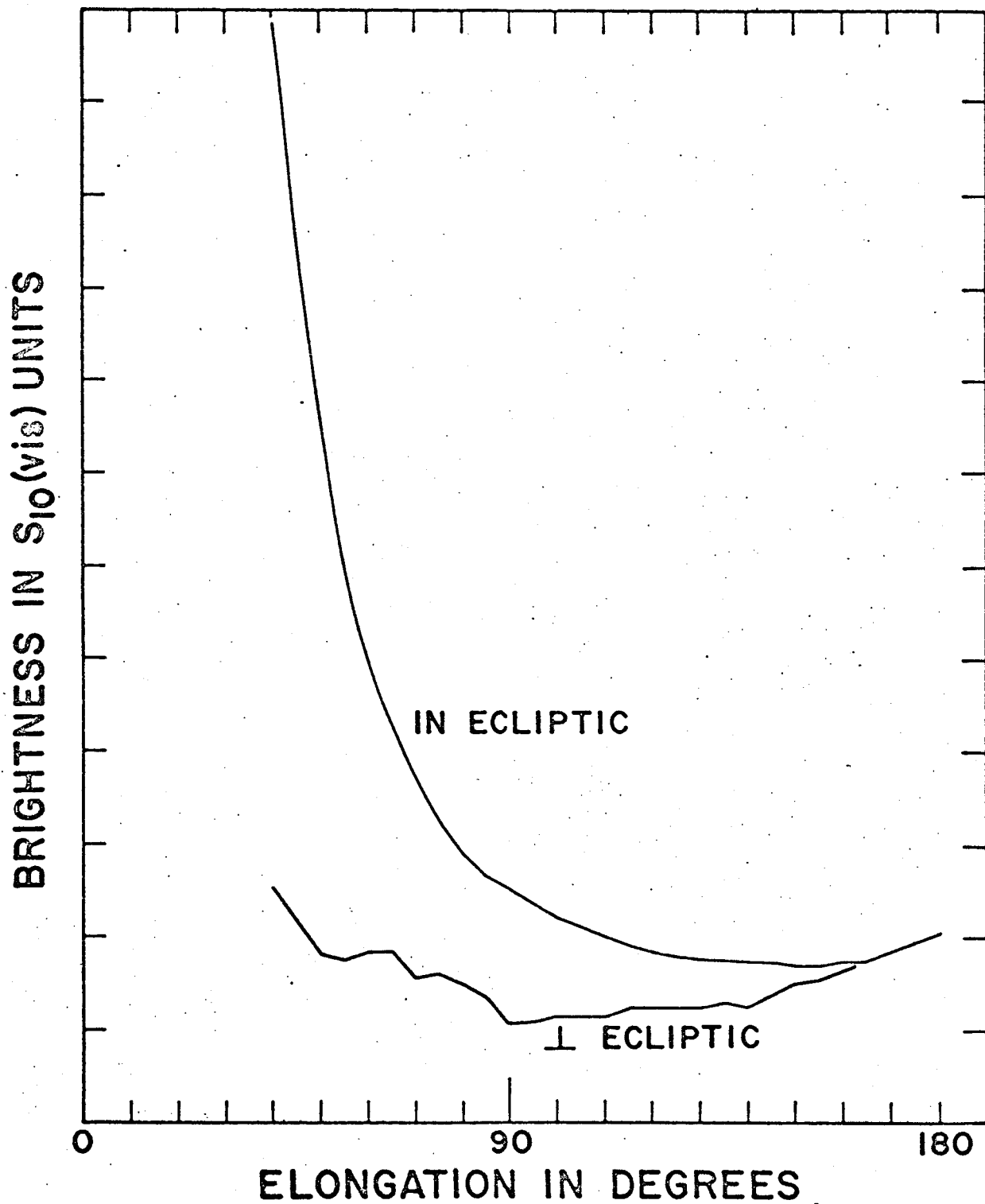| Elongation, ε	Brightness, S_{10}(vis)		Ratio, P.
	In ecliptic	⊥ ecliptic	
95	235	110	2.14
100	220	115	1.91
105	210	115	1.83
110	200	115	1.74
115	190	125	1.52
120	185	125	1.48
125	180	125	1.44
130	175	125	1.40
135	175	130	1.35
140	175	125	1.40
145	175	140	1.25
150	170	150	1.13
155	170	155	1.10
160	175	165	1.06
165	175	175	1.00
170	185	185	1.00
175	195	195	1.00
180	205	205	1.00

* From Richard et al.(11).
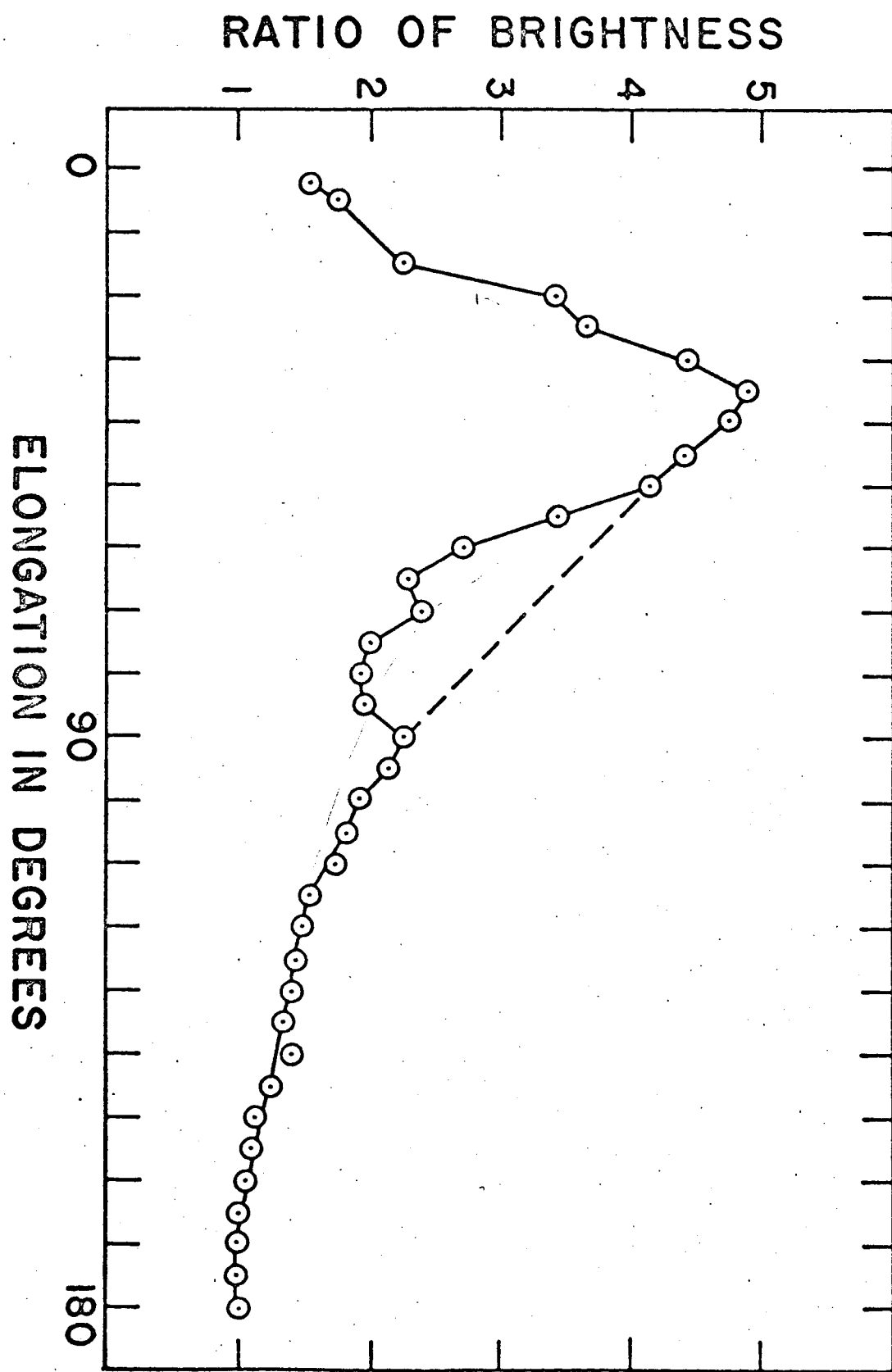** From Ingham(8) (Table III) multiplied by 1.20.

LEGEND FOR FIGURES

Fig. 1.   Isophotal map of the zodiacal light in polar coordinates.
The circumference represents the plane of the ecliptic with
values of differential longitude, $\lambda - \lambda_\odot$, increasing from $0°$
to $90°$ to $180°$ (the gegenschein). The ecliptic latitude, β ,
increases from $0°$ at the ecliptic to $90°$ in the center of the
circle.

Fig. 2   Brightness of the zodiacal light as a function of ecliptic
latitude for an elongation of $90°$.

Fig. 3   Brightness of the zodiacal light as a function of the
elongation for two planes: above in the ecliptic, below
at right angles to the ecliptic. The gegenschein is the
slight rise at $\epsilon = 180°$.

Fig. 4   Ratio of brightness of the zodiacal light in the ecliptic
to that in a plane at right angles to the ecliptic as a
function of elongation from the entries in Table 7.

Fig. 5   Brightness of the zodiacal/light as a function of differential
longitude for ecliptic latitudes ranging from $25°$ to $80°$.
The successive curves are displaced from each other by
50 S_{10}(vis) units.

Fig. 6   Brightness of the excess zodiacal light in a plane perpendi-
cular to the ecliptic as a function of elongation. The excess
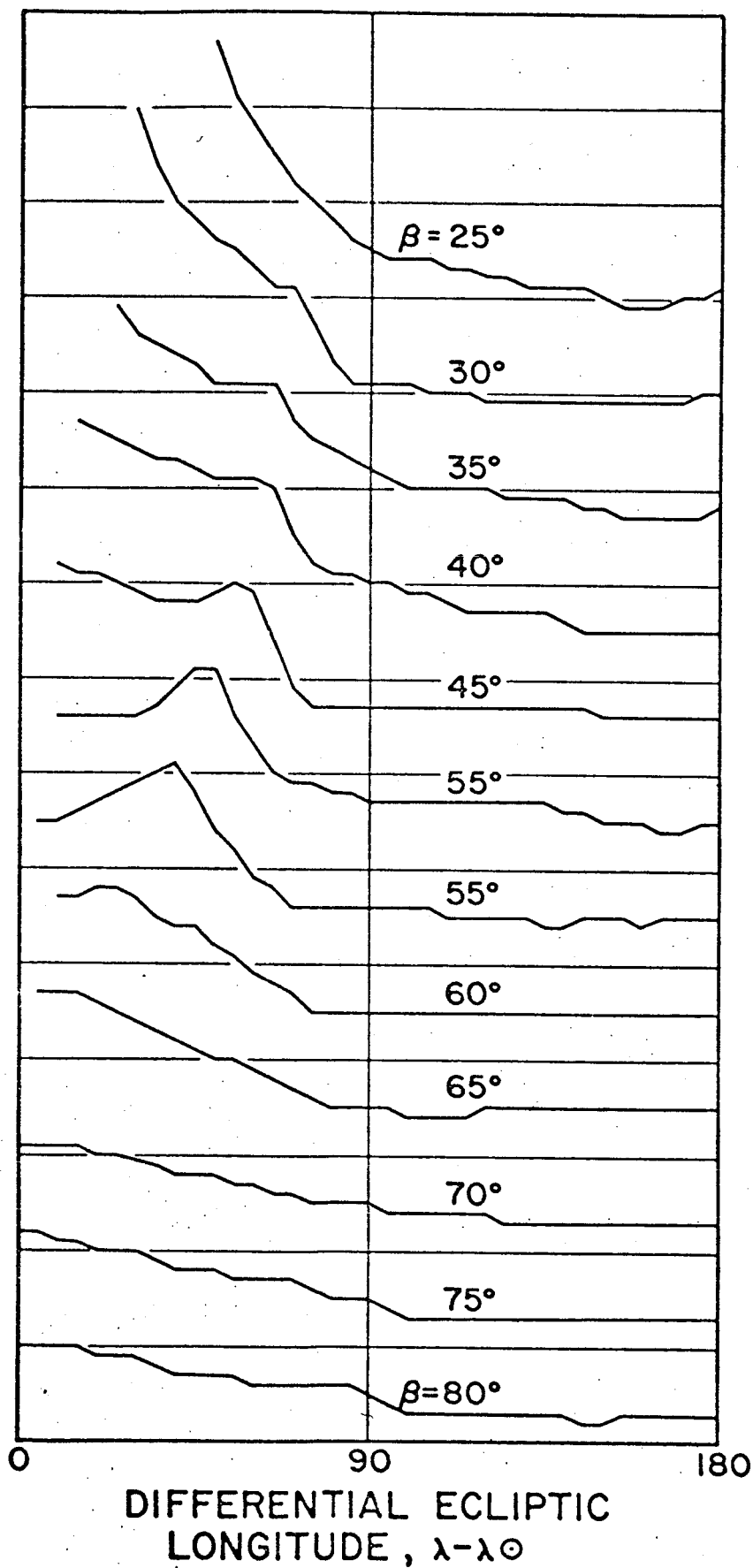is thought to be due to a terrestrial component (see text).

DIFFERENTIAL ECLIPTIC LONGITUDE, $\lambda-\lambda_\odot$

Figure 6